

Residual stresses measurement in the butt joint welded metals using FSW and TIG methods

Fathollah Taheri-Behrooz ^{*1}, Mohammad R.M. Aliha ², Mahmood Maroofi ¹ and Vahid Hadizadeh ¹

¹ School of Mechanical Engineering, Iran University of Science and Technology, Tehran, 16846-13114, Iran

² Welding and Joining Research Centre, School of Industrial Engineering, Iran University of Science and Technology (IUST), Narmak, 16846-13114, Tehran, Iran

(Received March 5, 2018, Revised June 18, 2018, Accepted July 5, 2018)

Abstract. Friction Stir Welding (FSW) is a solid-state process, where the objects are joined together without reaching their melting point. It has been shown that this method is a suitable way to join dissimilar aluminium alloys. The current article employed hole drilling technique to measure the residual stress distribution experimentally in different zones of dissimilar aluminium alloys AA6061-T6 and AA7075-T6 Butt welded using FSW. Results are compared with those of similar AA6061-T6 plates joined using a conventional fusion welding method called tungsten inert gas (TIG). Also, the evolution of the residual stresses in the thickness direction was investigated, and it was found that the maximum residual stresses are below the yield strength of the material in the shoulder region. It was also revealed that the longitudinal residual stresses in the joint were much larger than the transverse residual stresses. Meanwhile, Vickers micro hardness measurements were performed in the cross-section of the samples. The largest hardness values were observed in the stir zone (SZ) adjacent to the advancing side whereas low hardness values were measured at the HAZ of both alloys and the SZ adjacent to the retreating side.

Keywords: friction stir weld; TIG welding; residual stress measurement; hole drilling method; AA6061; AA7075; similar and dissimilar butt joints

1. Introduction

Some papers have been published up to now to measure the induced residual stresses (RS) inside the FSWed or fusion welded joints. For example, Castro *et al.* (2011) determined the residual stress field for a T-Joint made of AA 6056 and AA 7075 alloys using the central hole drilling (CHD) method. They showed that the RS field between the TMAZ and HAZ regions could be described well by using a logarithmic curve and the maximum residual tensile and compressive stresses induced due to the FSW process was equal to 100 MPa and 40 MPa, respectively. Aval *et al.* (2012) analyzed numerically a dissimilar AA 5086-AA 6061 FSW joint in the ABAQUS code and obtained a thermomechanical response and residual stress field around the weld line. They also compared their numerical RS data with experimental results available for some joints determined using the CHD method. According to their finding, while the pin rotational speed influences significantly on the maximum value of RS, the linear speed of tool can affect the distribution of transverse RS. Moreover, based on their experimental data the transverse RS value was about 40 to 60% of the corresponding longitudinal RS for the investigated FSW joint that was obtained using the CHD technique. Ting and Qing-yu (2008) measured the RS value in AA 2024-T6 welded plate

with a thickness of 3 mm and concluded that the value of longitudinal RS is greater than the transverse RS. The highest longitudinal RS value in the investigated aluminium plate was found about 164.5 MPa. Aliha and Gharehbaghi (2017) have recently computed numerically the induced residual stress field during gas tungsten arc welding of a thin aluminium cylinder manufactured by longitudinal seam weld. They investigated the influence of such residual stress on the fracture parameters of a semi-elliptical crack initiated in the weld line. Richter-Trummer *et al.* (2011) determined experimentally the RS field in a 3 mm thick FSWed AA 6082-T6 plate using the contour method. For validation of the employed experimental technique, they also compared the RS values with the CHD method and concluded that very good agreement exists between the results of both experimental RS measuring (i.e., contour and CHD) techniques. In another research, Jamshidi aval (2015) studied experimentally the influence of heat input on the RS field and microstructure of dissimilar AA 7070-T6 / AA 6082-T6 joint welded by the friction stir welding method. Jonckheere *et al.* (2013) investigated experimentally the influence of some parameters like temperature, applied torque and tool offset on the mechanical properties of similar and dissimilar FSW joints made of AA6061-T6 and AA2014-T6 plates having a thickness of 4.7 mm. The FSW residual stress effect on fatigue crack growth behavior of AA 2024-T351 alloy was investigated by Zhang *et al.* (2015). Zhou *et al.* (2015), designed a novel cooling system for reducing the value of RS during friction stir welding. Linton and Ripley (2008) determined the RS field in the

*Corresponding author, Professor,
E-mail: taheri@iust.ac.ir

FSWed 7xxx aluminium series via neutron diffraction technique. They showed that the values of RS decreases by time in both weld zone and HAZ after the welding. Similarly, using the neutron diffraction method, Xu *et al.* (2011) showed that the angular distortion of welding sample could affect the distribution of the generated heat by the shoulder of tool that results in uniform distribution of RS along the thickness. Wei *et al.* (2013) investigated the effect of tool pin depth on friction stir lap welding of aluminium to stainless steel. Effect of welding speed on the mechanical properties and strain-hardening behavior of friction stir welded 7075 Aluminium alloy joints was performed by Xu *et al.* (2017). Çam and Mistikoglu (2014), critically reviewed the recent developments in friction stir welding of Al-alloys. Residual stress in other metals is performed by many researchers as (Shigeru *et al.* 2004, Li *et al.* (2015) and Miroslav 2012).

In the current research, distribution of residual stress field for similar and dissimilar plates made of AA6061-T6 and 7075-T6 alloys butt-welded by the friction stir welding (FSW), and gas tungsten arc welding (TIG) methods are obtained experimentally. For this aim, the CHD method is utilized for measuring the values of longitudinal and transverse RS for different distances from the weld centreline. In addition, the variations of RS values along the thickness direction are determined using the incremental hole drilling technique. The micro hardness values in the weld zone for both welding methods are determined experimentally as well.

2. Experimental procedure

In this section procedures used for joining the aluminium alloys and the measuring procedure of the residual strains are explained in details.

2.1 Materials and welding methods

Two aluminium alloys (i.e., AA 7075-T6 and AA 6061-T6) were utilized in the current research and joined using FSW and GTAW (or TIG) methods. Accordingly, three plates with dimensions of $150 \times 150 \times 6$ mm³ were prepared. Chemical and mechanical properties of used aluminium alloys have been illustrated in Table 1.

For FSW joining of these two alloys, the plates were placed inside the welding fixture as schematically shown in Fig. 1. A cylindrical pin with a diameter of 10 mm and height of 6 mm were used as the welding tool. The diameter of shoulder and its concavity angle also considered equal to 20 mm and 6°, respectively. The welding tool was made from heat-treated H13 steel. For obtaining a sound FSW

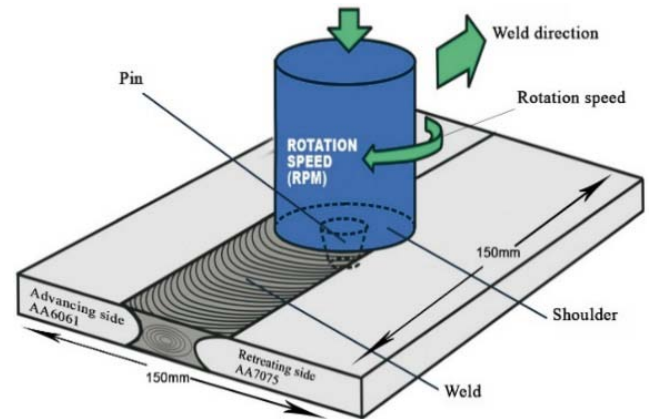


Fig. 1 A schematic view of the FSW process (Richter-Trummer *et al.* 2011)

joint, it is necessary to choose suitable input parameters such as tool tilt angle, transverse and rotational speeds of the tool, placing the plates at advancing and retreading sides, etc. The AA 7075-T6 was placed at advancing side and the AA 6061-T6 was placed at retreading side, respectively. This is mainly because, based on the previous works and observations in this regard that when the softer metal is placed at the retreading side, the transfer of this material to the advancing side becomes easier and results in better mixing of two alloys and good quality for the FSWed joint (Guo *et al.* 2014 and Aliha *et al.* 2016).

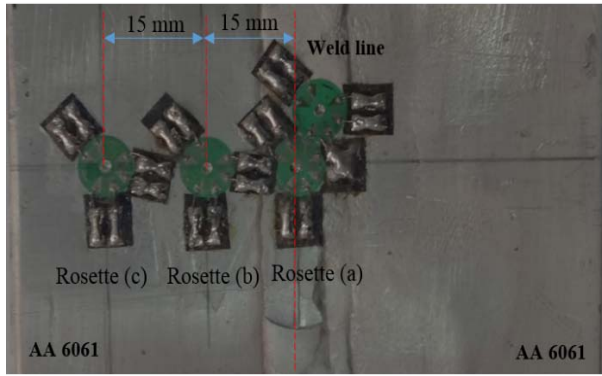
The transverse and rotational speeds of the mill machine utilized for joining the aluminium plates were 60 mm/min and 1115 mm/min, respectively. The tilt angle of the tool was also equal to 3°. Accordingly, three bi-metal AA 7075-T6 and AA 6061-T6 butt joints were manufactured successfully using the FSW technique and the quality of each joint was checked via visual inspection of the surface, optical microscopy and scanning electron microscopy (SEM) analyses. Also, three similar AA 6061-T6 butt jointed plates were manufactured using the same plate dimension but by the TIG method which is a conventional fusion welding technique for joining the weldable aluminium alloys like 6XXX series. An aluminium TIG welding wire (Al-Mg5 5356) was used as filler material during TIG welding.

2.2 Principal of the hole drilling method

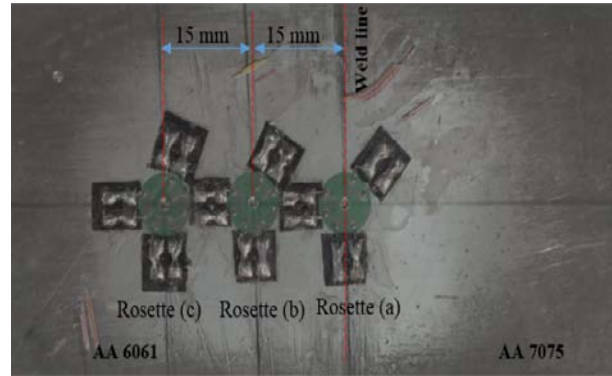
The hole-drilling method is a practical and widely used technique for determining residual stresses near the surface of a wide range of materials such as metals and composites. It consists of attaching a rosette strain gauges to the surface, drilling a hole through the rosette center in depth increments, and measuring the released strains. Finally, a set of equations are used to calculate the residual stresses. This test method is considered as “semi-destructive” because the induced damage does not affect the global behavior of the component. As specified by the ASTM E837-08 standard, this test method is limited to those cases where the maximum residual stresses do not exceed 50% of the material yield stress. Schajer (1981) employed finite element method to simulate hole drilling process

Table 1 Mechanical properties of the base material from tensile tests

Alloy	Yield strength (MPa)	Ultimate strength (MPa)	Hardness (Hv)
AA7075-T6	498	560	150
AA6061-T6	276	310	95



(a)



(b)

Fig. 2 Three rosette strain gauges type FRS-2-23 mounted on specimens of: (a) TIG; and (b) FSW

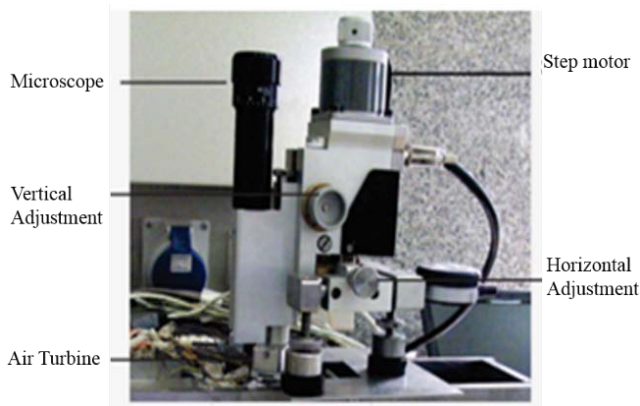


Fig. 3 The drilling system setup

numerically. He introduced calibration coefficients of A and B . Later Schajer (1988) presented modified coefficients \bar{a} and \bar{b} which were independent of the material property. Ghasemi *et al.* (2014) employed integral hole drilling method to measure non-uniform residual stress in orthotropic materials. Using contour method Liu and Yi (2013) obtained residual stress field in AA6061-T6 aluminium alloy joining by friction stir butt welds.

In the current research, the non-uniform residual stresses measurement procedure described in ASTM E837 standard is employed for measuring the residual stress variations in a depth of 1 mm from the surface of the welded samples. As shown in Fig. 2, three rosette strain gauges (type FRS-2-23 provided by TML Co.) were mounted on top of each specimen to record strain and subsequently residual stress of the whole field. The mechanical setup of the drilling system is shown in Fig. 3. It is a MTS 3000 system developed by SINT technology which allows holes to be drilled at a speed of 300,000 RPM. This speed minimizes local heating and residual stresses induced in the material to be analyzed as explained by Flaman *et al.* (1987). This system uses an optical microscope to align the drilling cutter exactly in the center of the rosette. The zero depth was automatically detected by the electrical contact technique. The feed rate, maximum depth, number of drilling steps, and delay time are set to 0.05 mm, 1 mm, 20, the 60 s, respectively, in compliance with standard ASTM E837-08. The strain values are measured using the three

element rosette gauges at each drilling step automatically, then strain variables p , q , and t are calculated as follows

$$p = \frac{\varepsilon_1 + \varepsilon_3}{2} \quad (1)$$

$$q = \frac{\varepsilon_3 - \varepsilon_1}{2} \quad (2)$$

$$t = \frac{\varepsilon_1 + \varepsilon_3 - 2\varepsilon_2}{2} \quad (3)$$

where ε_1 , ε_2 and ε_3 are the released strain components of each drilling step. The residual stresses are calculated for each hole depth step using the following equations

$$\bar{a}P = \frac{Ep}{1 + \nu} \quad (4)$$

$$\bar{b}Q = Eq \quad (5)$$

$$\bar{b}T = Et \quad (6)$$

where the stress components P , Q , and T are calculated from p , q , and t with the following equations

$$P = \frac{\sigma_1 + \sigma_2}{2} \quad (7)$$

$$Q = \frac{\sigma_2 - \sigma_1}{2} \quad (8)$$

$$T = \tau_{13} \quad (9)$$

where the numerical values of the calibration coefficients \bar{a} and \bar{b} for non-uniform residual stress evaluations are specified by the ASTM E837-08. E and ν are the Young's modulus and Poisson's ratio of the component. Also, σ and τ are normal and shear stress-components, respectively.

Finally, Eq. (10) is used to obtain principal stress components in each depth step, k .

$$(\sigma_{max})_k, (\sigma_{min})_k = P_k \pm \sqrt{Q_k^2 + T_k^2} \quad (10)$$

The angle between the maximum principal stress σ_{\max} and the strain gauge 1 direction, β , is calculated using the following equation

$$\beta_k = \frac{1}{2} \tan^{-1} \left(\frac{T_k}{Q_k} \right) \quad (11)$$

2.3 Micro hardness

In order to calculate the micro hardness of welded plates, the transverse section of welded plates were prepared according to the standard metallographic procedures and etched using a solution of Kellers etch (190 ml distilled water, 5 ml Nitric acid 65%, 5 ml Hydrochloric acid 32% and 1 ml Hydrofluoric acid 40%). The micro hardness of polished and etched specimens were measured at 1 mm distance from the top surface in steps of 1 mm by means of a Vickers micro hardness testing machine and by applying a load of 100 gr for 15 s. During the FSW process of heat treatable and non-heat-treatable aluminium alloys, a softening region is created in the weld zone especially for those alloys that heat treated under T6 condition. This behavior is mainly due to coarsening and dissolution of strengthening precipitates induced by heat generated in the TMAZ and HAZ regions. Consequently, a “W” shape

distribution is expected to observe in general for distribution of hardness in aluminium alloy since the FSW input parameters like pin geometry, temperature, welding force, type of welded materials and etc. can affect noticeably the size of grains in different locations along the weld section which changes the value of hardness.

3. Results

3.1 Residual stresses

The nature of these stresses in the welded region is mostly tensile. The magnitude of residual stress can be as high as the yield strength of the material. Also, it is highly dependent on the yield strength of the parent material. In general, high-strength materials possess a higher level of residual stress as shown by Lemmen (Lemmen *et al.* 2010). The 7XXX alloys have higher yield stress than 6XXX alloys. Hence, the level of residual stress in the 7XXX alloys should be higher than that of the 6XXX alloys. The specimens were drilled using depth increments of 0.05 mm to achieve a hole with final depth of 1 mm and 20 increments were made during drilling of each hole.

According to ASTM E837-08, the final hole depth was

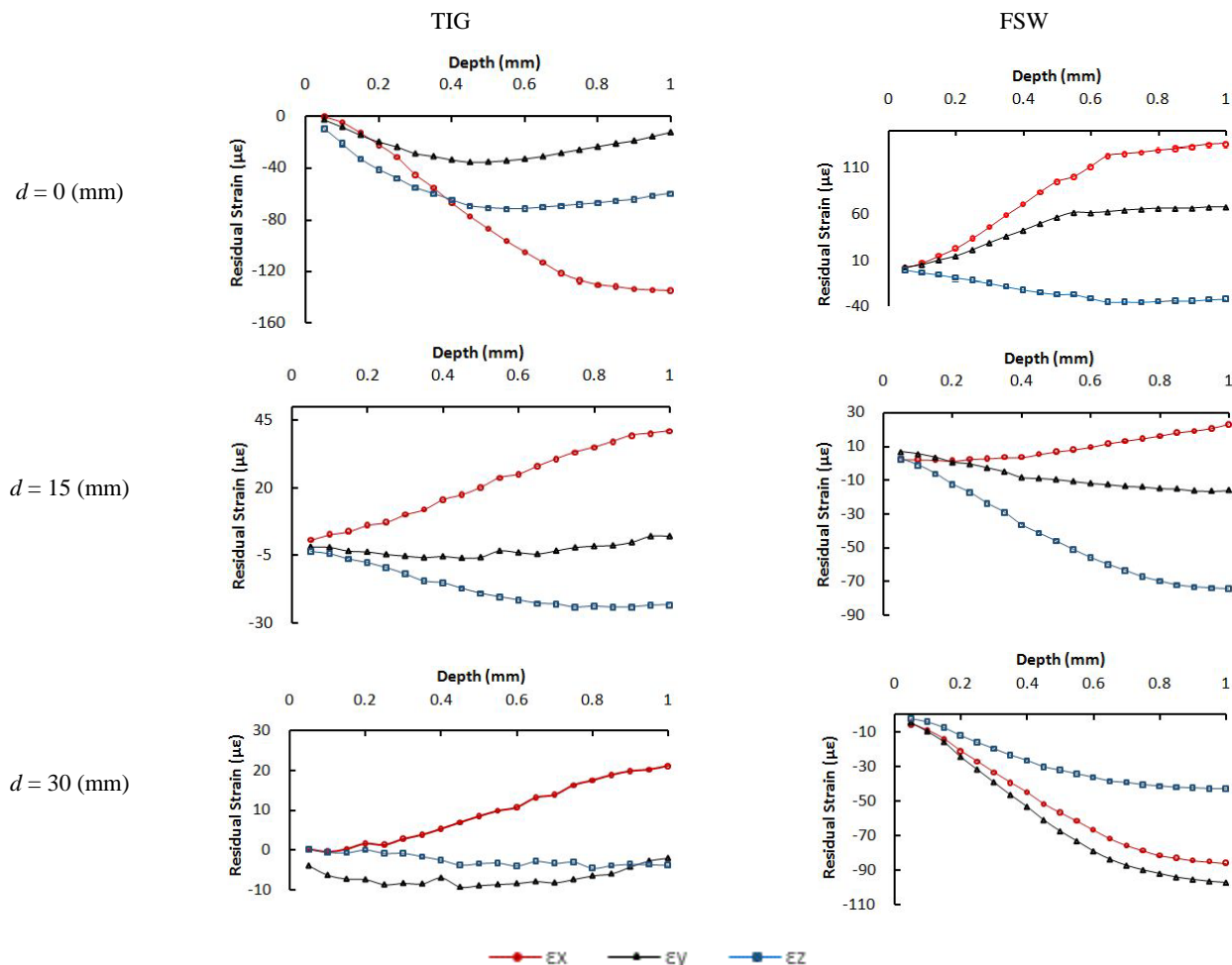


Fig. 4 The residual strain distribution in the specimens joined by TIG (left) and FSW (right) method in various distances from the weld centreline versus depth

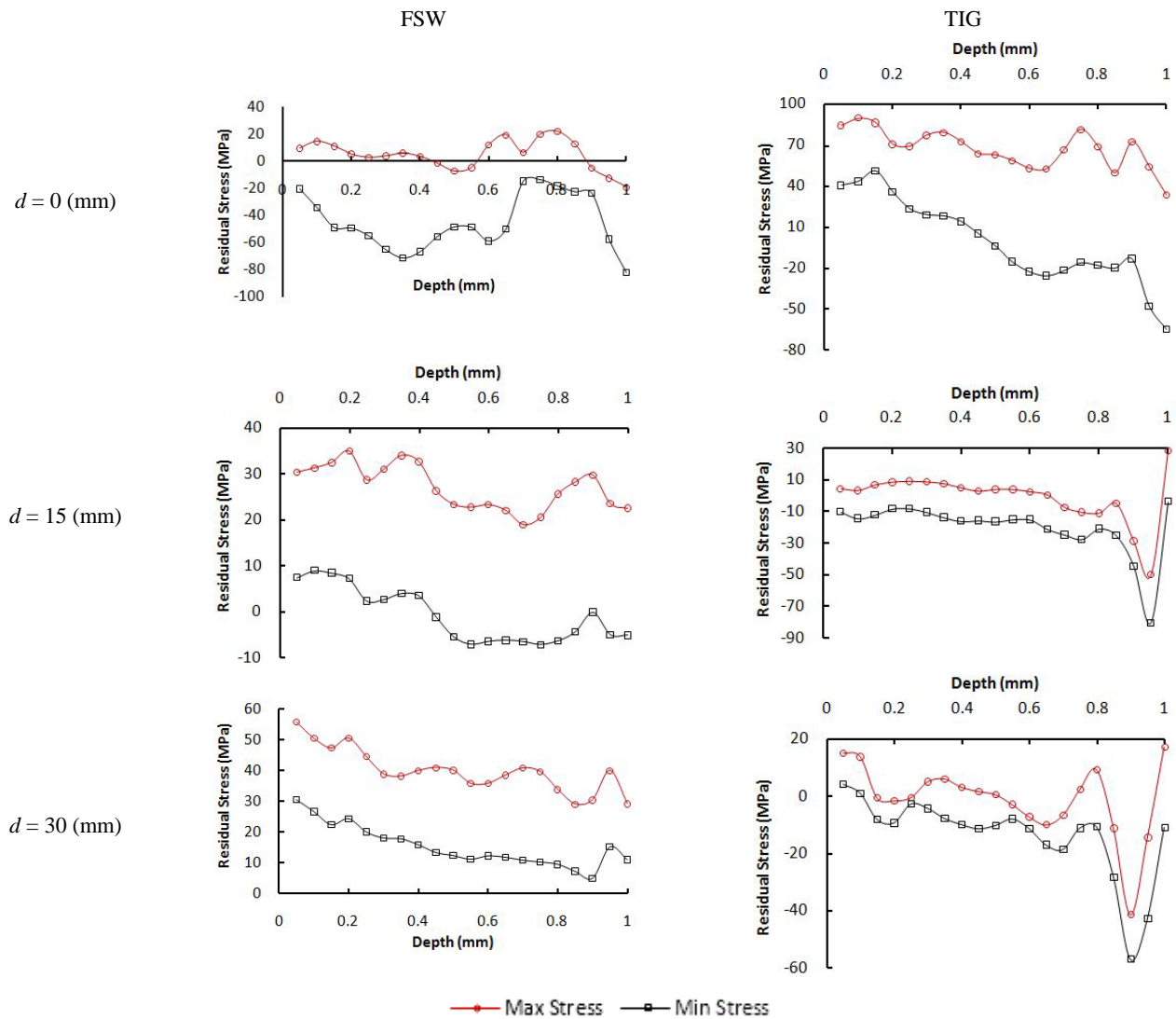


Fig. 5 Variations of the maximum and minimum residual stress in a length of d from the weld center line in FSW (left) and TIG (right) specimens

set at $0.2D$ or $0.24D$, where D is the rosette hole diameter. This would support to reduce the local stress concentration effects and allows residual stress measurements to be made to stresses up to 80% of the material yield stress.

Fig. 4 shows the distribution of the released residual strains (ε_1 , ε_2 , ε_3) in depth of the specimens for the six rosette strain gages which were installed according to Fig. 2. Released strains through thickness are affected by the both trapped stresses within a fixed increment and stresses within successive increments of a hole. However, the relieved strains are mostly influenced by the near-surface residual stresses. The effect of interior stresses decreases with their depth from the surface. Thus, hole drilling measurements can evaluate only near-surface stresses; deep interior stresses cannot be identified reliably. As shown in Fig. 4 the maximum released strain belongs to the rosette "a" in TIG welded samples, and its associated value is -160 micro strain. By getting away from the weld centreline, its value was decreased. Eq. (10) is used to calculate the maximum and minimum residual stresses for all rosettes in each drilling increment as shown in Fig. 5.

In FSW due to the heat generated by contact of the pin shoulder beneath with work pieces and also due to the temperature gradient of the surfaces, residual stress was reduced by depth increasing as shown in Figs. 5(d-f). As depicted in Fig. 5(f), in FSW the critical stress is tensile, and its value is about 56 MPa which was decreased with depth increasing. Also, its value was increased by getting away from the weld centreline. In TIG welding high-temperature gradient and maximum residual stress occur in the weld line as shown in Fig. 5(a). The maximum residual stress on the surface was about 90 MPa which was decreased by depth increasing and reached around 35 MPa at a depth of around 0.9 to 1 mm. By getting away from the weld line the value of the maximum and minimum stress reduces and tends to zero. Due to the technical limitations of the hole drilling method, the reported residual stresses of all positions at the final increment are not reliable as shown in Fig. 5. The findings of this research are in line with those reported by Sedighi *et al.* (2011). They investigated the calibration coefficients for non-uniform residual stress using finite element method and verified their findings with

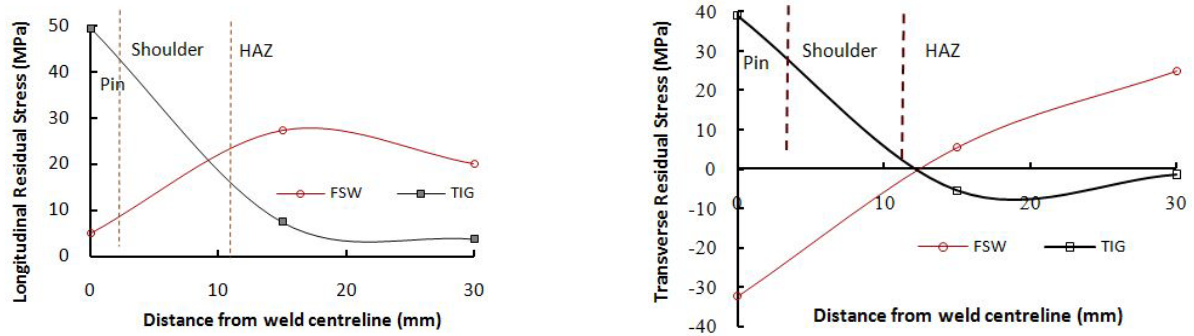


Fig. 6 Longitudinal (left) and transverse (right) residual stress for the specimens joined using FSW and TIG methods

theoretical values. They observed that the maximum depth through which the stress distribution can be determined accurately is limited by some reasons, such as, error in strain gage bonding and stress concentration effects due to the drilled hole.

During the TIG welding, residual stresses were developed from two sources, the dimensional change of the material volume due to solidification shrinkage and mechanical compressive strain due to solidified welded material's interaction with surrounding material during the cooling cycle. However, in FSW, the compressive plastic strain accumulated during heating and cooling cycle leads to the overall development of residual stresses. For this reason, the magnitude of residual stress in some cases of FSW components is comparable to that in TIG components even though peak temperatures are significantly different.

As shown in Fig. 6 (left) for FSW samples longitudinal residual stress in the center of the weld has tensile nature and away from the weld center first increases up to maximum tensile stress near the edge of the tool then in the farther distance is decreased. The lower stress magnitude of the weld centreline may be explained by the change in microstructure and hardness of the weld nugget zone due to recrystallization of the grains as explained by Aval (2015). The heavily worked grains of the weld nugget cause stresses to be relieved as the material cools down after welding. Away from the weld centreline where the material is not affected by the stirring action of the tool, the stresses are nearly zero. Meanwhile, as shown in Fig. 6 (right) in the weld center line, the transverse stress of FSWed samples has compressive nature, and its maximum value was occurred in farther distance compared to the position of the maximum longitudinal residual stress.

As depicted in Fig. 6 (left), for TIG joints longitudinal residual stress in the center of the weld has tensile nature and is maximum which was decreased by getting away from the weld centreline. The overall behavior of transverse residual stress (Fig. 6 (right)) is similar to the longitudinal residual stress in the TIG welded specimens. The transverse stress experienced its maximum value at the weld center then decreased and became compressive by getting away from the weld center. The maximum longitudinal residual stress for the TIG weld is 50 MPa in the weld line, and for the FSW weld is 30 MPa which is away from the weld center, and its value at the center line is 5 MPa that causes further distortion in the TIG welded specimens.

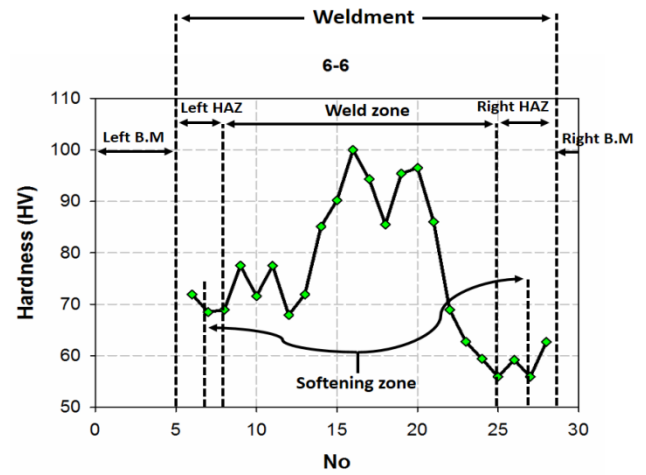


Fig. 7 The micro-hardness profiles of similar (AA 6061-T6) joints welded by the TIG method

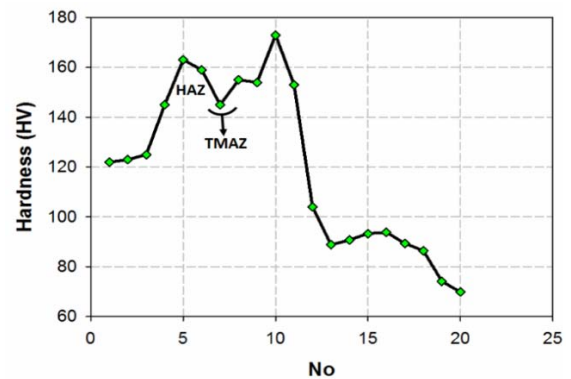


Fig. 8 The micro-hardness profiles of dissimilar (AA 6061/AA 7075 T6) joints welded by the FSW

3.2 Micro hardness

Figs. 7 and 8 show the micro-hardness profiles obtained from the cross-section of similar AA 6061-T6 and dissimilar (AA 6061-T6/AA7075-T6) joints welded by the FSW and TIG methods. As seen from Fig. 7, the average hardness of welded zone is higher than both base metal and HAZ mainly due to high residual stress induced during the solidification phase. The value of hardness in the HAZ region is reduced drastically because of enlargement of

grains demonstrating the softening behavior of the material in this region. The increased hardness value in that region of AA 6061-T6 TIG welded zone in Fig. 7 is mainly due to Mg₂AlFeSi dissolutions. Meanwhile, low rate of heat input and lower values of residual stresses induced by welding results in significantly low hardness value for the base metal in comparison with the weld zone of AA 6061-T6 joint manufactured with fusion welding TIG method. The points 1 to 11 in micro-hardness profile presented in Fig. 8 are related to AA 7075-T6 alloy, and the rest of points describe the hardness of AA 6061-T6 alloy for different locations from the weld center of dissimilar AA 6061-T6 and AA 7075-T6 joint. The nugget zone which is located at the interface of dissimilar joint lies between points 11 and 12. The stir zone of Al 7075-T6 that has the highest hardness value also lies between points 8 to 11. Point 7 presents the reduced hardness of TMAZ zone in AA 7075-T6 alloy. It is also seen from Fig. 8 that after point 12, the hardness is reduced drastically demonstrating switch of the material from harder material (i.e., AA 7075-T6) to the softer one (i.e., AA6061-T6).

4. Conclusions

- Residual stress (RS) fields induced by two welding methods (i.e., TIG and FSW) in similar and dissimilar aluminium alloys were determined experimentally using central hole drilling (CHD) technique.
- While the RS value was decreased by moving the weld line and tended to zero for joint made by fusion welding (TIG) technique, the value of RS in the solid state friction-stir welding (FSW) was first increased relative to the weld line and then reduced by moving towards the far distances from the weld line. Indeed, the maximum RS value in the fusion welding is obtained exactly at the centreline of the weld, but for the case of FSW joint, its maximum was reached at a certain distance from the weld line depending on the shoulder diameter.
- The residual stress (RS) values induced during the FSW welding method was significantly smaller than those of the TIG method.
- Variations of hardness along the weld section of dissimilar AA7075-T6/ AA6061-T6 joint and similar AA6061-T6 joint were obtained. It was found that the hardness of weld zone is higher than the base metal in the weldments.

References

- Aliha, M.R.M. and Gharehbaghi, H. (2017), "The effect of combined mechanical load/welding residual stress on mixed mode fracture parameters of a thin aluminium cracked cylinder", *Eng. Fract. Mech.*, **180**, 213-228.
- Aliha, M.R.M., Shahheidari, M., Bisadi, M., Akbari, M. and Hossain, S. (2016), "Mechanical and metallurgical properties of dissimilar AA6061-T6 and AA7277-T6 joint made by FSW technique", *Int. J. Adv. Manuf. Tech.*, **86**(9-12), 2551-2565.
- Aval, H.J. (2015), "Microstructure and residual stress distributions in friction stir welding of dissimilar aluminium alloys", *Mater. Des.*, **87**, 405-413.
- Aval, H.J., Serajzadeh, S. and Kokabi, A.H. (2012), "Experimental and theoretical evaluations of thermal histories and residual stresses in dissimilar friction stir welding of AA5086-AA6061", *Int. J. Adv. Manuf. Tech.*, **61**(1-4), 149-160.
- Çam, G. and Mistikoglu, S. (2014), "Recent developments in friction stir welding of Al-alloys", *J. Mater. Eng. Perform.*, **23**(6), 1936-1953.
- Castro, R.A.S., Richter-Trummer, V., Tavares, S.M.O., Moreira, P.M.G., Vilaça P. and de Castro, P.M.S.T. (2011), "Friction stir welding on T-joints: residual stress evaluation", *Mecânica Experim.*, **19**, 55-65.
- Choi, D.H., Lee, C.Y., Ahn, B.W., Yeon, Y.M., Park, S.H.C., Sato, Y.S., Kokawa, H. and Jung, S.B. (2010), "Effect of fixed location variation in friction stir welding of steels with different carbon contents", *Sci. Technol. Weld. Join.*, **15**(4), 299-304.
- Flaman, M.T., Mills, B.E. and Boag, J.M. (1987), "Analysis of stressvariation-with-depth measurement procedures for the center-hole method of residual stress measurement", *Exp. Techniq.*, **11**(6), 35-37.
- Ghasemi, A.R., Taheri-Behrooz, F. and Shokrieh, M.M. (2014), "Determination of non-uniform residual stresses in laminated composites using integral hole drilling method: Experimental evaluation", *J. Compos. Mater.*, **48**(4), 415-425.
- Guo, J.F., Chen, H.C., Sun, C.N., Bi, G., Sun, Z. and Wei, J. (2014), "Friction stir welding of dissimilar materials between AA6061 and AA7075 Al alloys effects of process parameters", *Mater. Des.*, **56**, 185-192.
- Jonckheere, C., de Meester, B., Denquin, A. and Simar, A. (2013), "Torque, temperature and hardening precipitation evolution in dissimilar friction stir welds between 6061-T6 and 2014-T6 aluminium alloys", *J. Mater. Process. Technol.*, **213**(6), 826-837.
- Lemmen, H.J.K., Alderliesten, R.C., Pieters, R.R.G.M., Benedictus R. and Pineault, J.A. (2010), "Yield Strength and residual stress measurements on friction-stir welded aluminium alloys", *J. Aircr.*, **47**(5), 1570-1583.
- Li, T., Shi, Q.Y., Li, H.K., Wang, W. and Cai, Z.P. (2008), "Residual stresses of friction stir welded 2024-T4 joints", *Mater. Sci. Forum*, **582**, 263-266.
- Li, T.J., Liu, S.W. and Chan, S.L. (2015), "Cross-sectional analysis of arbitrary sections allowing for residual stresses", *Steel Compos. Struct., Int. J.*, **18**(4), 985-1000.
- Linton, V.M. and Ripley, M.I. (2008), "Influence of time on residual stresses in friction stir welds in agehardenable 7xxx aluminium alloys", *Acta Materialia*, **56**(16), 4319-4327.
- Liu, C. and Yi, X. (2013), "Residual stress measurement on AA6061-T6 aluminium alloy friction stir butt welds using contour method", *Mater. Des.*, **46**, 366-371.
- Miroslav, B. (2012), "Experimental investigation of residual stresses in cold formed steel sections", *Steel Comp. Struct., Int. J.*, **2**(6), 465-489.
- Richter-Trummer, V., Moreira, P.M.G. P. and Ribeiro, J. (2011), "The contour method for residual stress determination applied to an AA6082-T6 friction stir butt weld", *Mater. Sci. Forum*, **681**, 177-188.
- Schajer, G.S. (1981), "Application of finite element calculations to residual stress measurements", *J. Eng. Mater. Technol.*, **103**(2), 157-163.
- Schajer, G.S. (1988), "Measurement of non-uniform residual stresses using the hole-drilling method", *J. Eng. Mater. Technol.*, **110**(4), 338-343.
- Sedighi, M., Khandae, M. and Joudaki, J. (2011), "Calibration coefficients for residual stress measurement in incremental hole drilling method", *Modares Mech. Eng.*, **11**(1), 19-27.
- Shigeru, A., Tadashi, N. and Tetsumaro, H. (2004), "Reduction of

- residual stress for welded joint using vibrational load”, *Steel Comp. Struct., Int. J.*, **4**(5), 355-365.
- Wei, Y., Li, J., Xiong, J. and Zhang, F. (2013), “Effect of tool pin insertion depth on friction Stir lap welding of aluminium to stainless steel”, *J. Materi. Eng. Perform.*, **22**(10), 3005-3009.
- Xu, W., Liu, J. and Zhu, H. (2011), “Analysis of residual stresses in thick aluminium friction stir welded butt joints”, *Mater. Des.*, **32**(4), 2000-2005.
- Xu, W., Li, Z. and Sun, X. (2017), “Effect of welding speed on mechanical properties and the strain-hardening behavior of friction stir welded 7075 aluminium alloy joints”, *J. Mater. Eng. Perform.*, **26**(4), 1938-1946.
- Zhang, Z., Zhang, Z. and Zhang, H. (2015), “Effect of residual stress of friction stir welding on the fatigue life of AA 2024-T351 joint”, *Proceedings of the Institution of Mechanical Engineers, Part B; Journal of Engineering Manufacture*, **229**(11), 2021-2034.
- Zhou, X., Mackenzie, D. and Pan, W. (2015), “A new distributed cooling method for mitigating residual stress in friction stir welding”, *Proceedings of the Institution of Mechanical Engineers, Part B; Journal of Engineering Manufacture*.
DOI: 10.1177/0954405415573849